MODELLING THE ELASTIC STIFFNESS OF A DISCRETELY ASSEMBLED TOWER

Miana Smith
Massachusetts Institute of Technology
Cambridge, MA, USA

ABSTRACT

The production of complex objects with specific electro-mechanical properties can be made easier by using discretely assembled structures, i.e. structures made out of repeating, individual components. Current research on discretely assembly structures is typically limited to highly technical applications, though discrete assemblies can be especially useful in less specialized applications because of their simplicity to produce. To simplify the design process of these structures, a simple spring model was used to predict the elastic stiffness of a discretely assembled tower. The same geometries were tested under compression for four materials: stainless steel, medium density fiberboard, cast acrylic, and corrugated fiberboard. The actual stiffness of the tower assembly was then compared to the modelled stiffness of the tower. The modelled stiffness overlaps with the measured stiffness for MDF and acrylic, indicating potential use for materials in this stiffness range, while it is unable to predict the stiffness of steel and cardboard.

INTRODUCTION

Discretely assembled structures make manufacturing easier. They can be assembled and re-assembled almost endlessly, and the same set of parts can be used to create a variety of diverse structures, partially eliminating the need for highly specific and low volume manufacturing. Further, this strategy is accessible to a wider user base, as it extends the control of present "desktop" fabrication machines past their machine dimensions [1]. Additionally, it is possible to essentially program in desired electrical or mechanical properties into the final assembly through control of the geometry and material of the component parts [2].

The research around discretely assembled structures is in a relatively early state, with much of the current literature concerned with specific, complex applications, such as in developing lightweight airfoils [3, 4], or with the actual manufacturing processes associated with various material types [5, 6]. In contrast, this experiment seeks to characterize very basic mechanical properties, i.e. elastic stiffness, for an architecture without a specific application using simple physical concepts. The intention behind this experimental design is to clarify the aspects of discrete assembly design in a way that is more accessible to people with a general though non-specific technical background.

To assess the practicality of using simple physical concepts to predict the behavior of a discrete assembly, the measured elastic stiffness of an assembly is compared to a modeled elastic stiffness based on a spring model. A four-part repeating pattern is cut from 3.175mm thick steel, 3.175mm thick medium density fiberboard (MDF), 3.175mm thick acrylic, and C-flute corrugated fiberboard (approx. 4 mm thick). These materials were chosen because they represent a wide range of elastic stiffnesses, and are commonly used in digital fabrication because they are easy to machine and work with. For each material, a rectangular patch, the primary repeating components parts, and the tower assembly is tested under compression using either a Instron Universal Testing System or the Stable Microsystems TA.XT Plus, a texture analyzer (both machines are from the MIT Mechanics and Materials Lab, Cambridge MA). A modelled stiffness is calculated from the measured component stiffnesses and compared to the measured tower stiffness. Additionally, the effect of the geometry on the stiffness of each component can be compared across the materials. Together, these help to characterize the mechanical behavior of the tower and the validity of the spring model.

BACKGROUND

DISCRETELY ASSEMBLED STRUCTURES

Discretely assembled structures are able to achieve a high level of organization from an imprecise assembler because of the precision and self-correcting nature of their component parts. A classic example of this is a Lego™ Brick set, in which a child– an imprecise assembler– is able

to create a predictable, controlled, and complex structure. Further, given the same set of materials, a second child is presumably able to create the same object as the first child. The level of accuracy and precision reached by the final Lego™ architecture is predicated on the quality and nature of each individual brick. The kinematic connections between bricks are heavily constrained by the amount and arrangement of finger-slot adapters between each brick, and the consistency of these across different bricks is ensured by complex manufacturing and quality control processes [2]. This research is concerned with re-applying the Lego™ strategy to an industrial or architectural scale. Objects would be created by converting the target solid geometry into a lattice structure, which could then be made from a limited set of mass produced component parts. The behaviors of the final object can be finely tuned by varying the material and mechanical properties of the component parts, and their placement in the assembled structure.

MATERIAL SELECTION

The four materials used in this experiment represent both a wide range of material properties and some of the more common prototyping/manufacturing materials in the digital fabrication realm. They are useful for digital fabrication because they are simple to obtain and work with. Importantly for this study, each of these materials can be safely laser cut. The most stiff material is type 304 stainless steel, which is one of the most common steel alloys used because of its good machining and welding properties. It has a commonly reported Young's Modulus of 193 GPa [7]. Medium density fiberboard (MDF) is a wood based hardboard that is desirable for prototyping because of its relative strength and consistent cross section. It has a commonly reported Young's Modulus of 4 GPa [8, 9]. Cast translucent acrylic is a widely used plastic that is safe to laser cut. Because of its manufacturing process, it has a slightly greater variation in thickness compared to steel or MDF. It has a commonly reported Young's Modulus of 3.2 GPa [9,10]. Corrugated C-flute fiberboard, which is the cardboard likely most commonly seen used for packaging and shipping of small goods, is useful for digital fabrication because it is cheap and very simple to work with. C-flute fiberboard is also approximately 4 mm thick, which when slightly compressed can match the thickness of the other materials used in this study. In the cross direction, it has a commonly reported Young's Modulus of 0.26 GPa [11].

SPRING MODEL TOWER

Every test run in this experiment consists of axially loading a sample under compression and recording the load force (N) and the displacement of the part (mm), as shown in Figure 1.

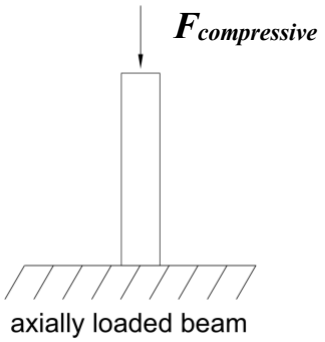

Figure 1: The testing set-up of the material tabs, component parts, and tower. Each part is treated as an axially loaded beam under compression and the elastic stiffness is determined from the equations that describe this behavior.

The simple tabs are rectangular prisms with a known, constant cross section, so the engineering stress-strain behavior of these parts can be determined from the load force versus displacement data generated from the Instron testing. The elastic stiffness (Young's Modulus) is given by the slope of the part's elastic regime (see Equation 1, where σ is stress, E is Young's Modulus, and ε is the engineering strain) [12].

$$\sigma = E\varepsilon \tag{1}$$

For the geometrically complex component parts, the spring stiffness, as given by Hooke's Law, is instead determined (see Equation 2, where F is force (in Newtons), k is the spring stiffness (in Newtons/millimeter), and x is the displacement (in millimeters) from equilibrium) [13].

$$F = -kx \tag{2}$$

The spring stiffness k can be extracted from the linear portion of the load-displacement graphs.

After determining the stiffness k of each component part, the overall stiffness of the tower can be predicted by approximating the tower as a series stack of four in parallel springs. Each building unit of the tower is approximated by two component parts of the b.) type, and two component parts of the a.) type, as labelled in Figure 3. See Figure 2 for a representation of the spring model.

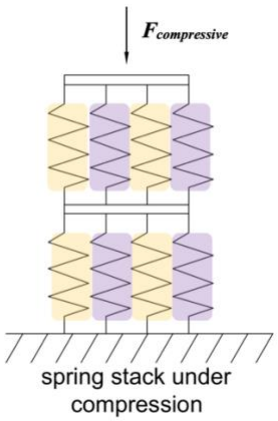

Figure 2: A representation of a two-unit tower assembly. Each component is represented by a spring, and each repeating unit of the tower is a set of four springs in parallel. The overall stiffness of the tower is represented by the equivalent stiffness of the series stack of springs. k_1 is highlighted in orange, while k_2 is highlighted in purple.

The equivalent stiffness of the tower can then be computed by Equation 3, where k_1 is the stiffness of one component type (highlighted orange), k_2 is the stiffness of the other (highlighted purple), and N is the number of repeating units in the tower (in this experiment, $N = 2$).

$$k_{eq} = \frac{2(k_1+k_2)}{N} \quad (3)$$

This model is an imperfect representation of the physical system– importantly, it does not acknowledge that the part types (and therefore springs) are staggered in height, and it treats the horizontal linking components as perfectly rigid. However, it provides a good starting point for comparing the theoretical tower stiffness to the actual tower stiffness.

EXPERIMENTAL DESIGN

TOWER DESIGN

The towers are assembled from four distinct cell types, which are shown in Figure 3. Pattern a.) and b.) in the figure form the primary repeating units of the tower, while c.) and d.) are used for the start and end caps of the tower. Pattern a.) is referred to as the "flexure" part and pattern b.) is the "square" part. The assembled tower that is tested in this project consists of one repeating unit, with a start and end cap. A 3-D model of this tower is shown in Figure 4. This tower represents the minimum height that includes all of the parts.

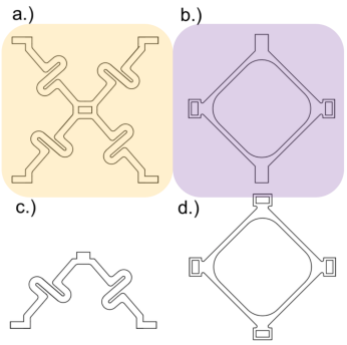

Figure 3: The four component part geometries. Pattern a.) (the flexure) and b.) (the square) link together to form the primary repeating units, while c.) and d.) are used as the start and end caps of the tower. Color coding is used here to help visually track the parts from the spring model through to the CAD model.

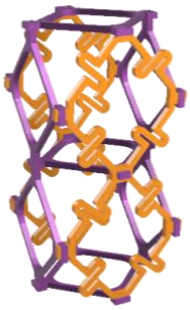

Figure 4: CAD model of the assembled tower. The component parts join to form a "cuboct" geometry, which is a structurally rigid geometry [14]. The flexural components are colored orange while the square parts are colored purple.

APPARATUS

The parts and tower are tested on either an Instron Universal Testing Machine with compressive grips and a 20000 lb. (9071kg) load cell or on a TA.XT Texture Analyzer with compressive grips and a 50N load cell. The cardboard parts and assembly are tested using the Texture Analyzer because the Instron UTM does not have the resolution to measure the load-displacement behavior of something as fragile as cardboard. Some of the acrylic and MDF components were also tested using the Texture Analyzer, for convenience. All of the other parts were tested using the Instron UTM. A diagram and photograph of the testing set-up is shown in Figure 5. The parts and tower assemblies are tested in the same method; they are tested under an axial, compressive load. Load (N) versus displacement (mm) data is collected for all of the test parts,

with a maximum displacement of between 2.5mm – 5mm. In the interest of characterizing the material's properties, a rectangular tab of each material is also compression tested. The simple geometry and constant cross-section of these tabs means that the engineering stress-strain behavior of the material can be extracted from the load-displacement data. Figure 4 shows a photo of the component parts and tabs that are individually tested. Only the square part and flexure part are compression tested. The other two components are excluded because the half-flexure part should behave similarly to the whole-flexure part, and the base caps are installed horizontally, and should therefore not contribute significantly to the elastic behavior of the full assembly.

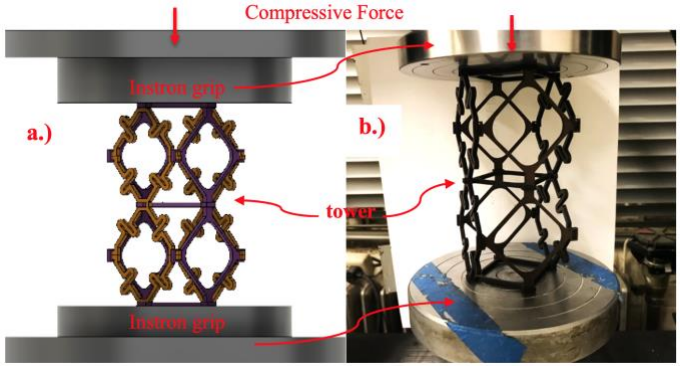

Figure 5: a.) A diagram and a b.) photo of the testing set up, with a tower assembly installed. The assembly or component part is placed between two compression grips on either the Instron Universal Testing Machine or the TA.XT Texture Analyzer and load (N) versus displacement (mm) data is collected. For the Instron UTM, a 20000lb (9071 kg) load cell is used, and for the Texture Analyzer, the default 50N load cell is used.

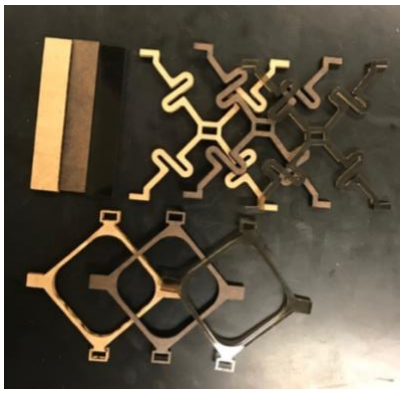

Figure 6: A photograph of the component parts and tabs that were load-displacement tested in addition to the tower. Three material types are shown here: cardboard, MDF, and acrylic.

Four material types are tested: 3.175mm stainless steel, 3.175mm medium density fiberboard (MDF), 3.175mm cast acrylic, and C-flute (~3 - 4mm thick) corrugated fiberboard. All of the parts, save the steel parts, are cut on a Universal Laser Systems laser cutter. The steel parts are cut on a FabLight laser cutter. The same part design is cut on all of the materials (see Figure 6 for tested part geometries). Even though the cardboard thickness is not the same as that of the other materials, the same cut file is still usable because the cardboard can be slightly compressed so that the press fit joints still work. The design is meant to hold together without additional joinery. The steel, MDF, and cardboard hold together without additionally fixing the joints. The acrylic parts are slightly looser because of differing laser cutter settings and larger manufacturing tolerances in the material thickness, so a small amount of cyanoacrylate adhesive was used at some of the joints to keep the tower more stable.

The data collected is analyzed through fitting a linear curve to the elastic portion of the response using LoggerPro and recording the slope with uncertainty as the elastic stiffness of the tested part. This workflow is illustrated in Figure 7. Each part is tested 3-7 times, and the reported stiffness is the averaged value with uncertainty.

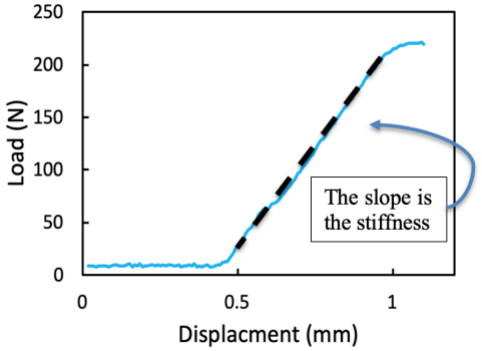

Figure 7: A selection of raw data with a linear fit over the elastic regime of the material's response. Only the slope of that part of the material response is relevant to this study. The initial flat line is caused by slack in the system, while the later plateau indicates that the material has entered its plastic regime.

RESULTS AND DISCUSSION

ELASTIC RESPONSE OF COMPONENT PARTS

The flexure part, as expected, is consistently less stiff than the square part, though to a varying degree. For steel, the square part was about 3 times as stiff as the flexure. For MDF, the square part was 2.5 times as stiff as the flexure. For acrylic, it was 1.6 times as stiff, and for cardboard the square part was 1.3 times as stiff. See Figures 8 through 11 for graphs of the component stiffnesses for all material

types as well as the actual stiffnesses of each part. The magnitude of the difference between these values increases as the material stiffness increases, which indicates that the effect of the geometry on the stiffness of the part is more apparent for stiff materials.

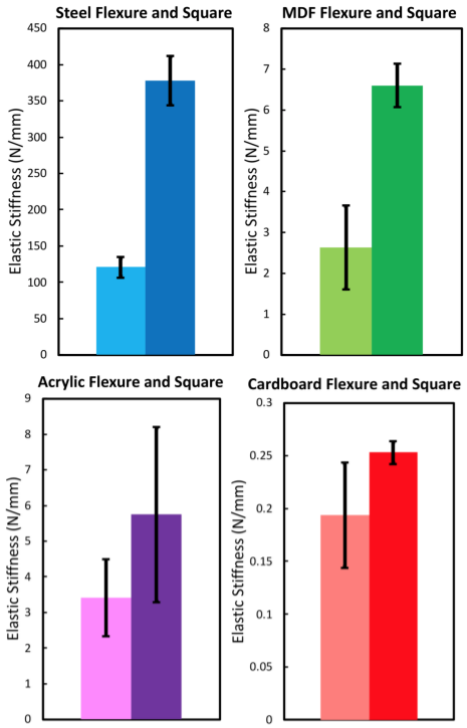

Figure 8: A graph of the average elastic response of the stainless steel, MDF, acrylic, and cardboard flexure and square parts. The elastic stiffness of the steel square part was (378 ± 33)N/mm and the elastic stiffness of the flexure was (120 ± 12)N/mm. The elastic stiffness of the MDF square part was (6.6 ± 0.5)N/mm and the elastic stiffness of the flexure was (2.6 ± 1.1)N/mm. The elastic stiffness of the acrylic square part was (5.7 ± 2.4)N/mm and the elastic stiffness of the flexure was (3.4 ± 1.1)N/mm. The elastic stiffness of the cardboard square part was (0.25 ± 0.01)N/mm and the elastic stiffness of the flexure was (0.19 ± 0.05)N/mm.

ELASTIC RESPONSE OF ASSEMBLED TOWERS

For MDF and acrylic, the spring model underestimates the stiffness of the actual tower, though the values do have overlap. For steel and cardboard, the model substantially overestimates the stiffness of the actual tower, and has no overlap with the measured value. A summary of the modelled tower stiffnesses and actual tower stiffnesses for all materials can be found in Table 1, while a graphs of these values can be found in Figure 9.

Table 1: Summary of the modelled tower stiffnesses and actual tower stiffnesses for all materials.

Material Type	Modelled Tower Stiffness (N/mm)	Actual Tower Stiffness (N/mm)
Steel	499 ± 46	293 ± 61
MDF	9.2 ± 1.5	12.8 ± 1.3
Acrylic	9.2 ± 3.2	9.6 ± 0.6
Cardboard	0.45 ± 0.06	0.26 ± 0.01

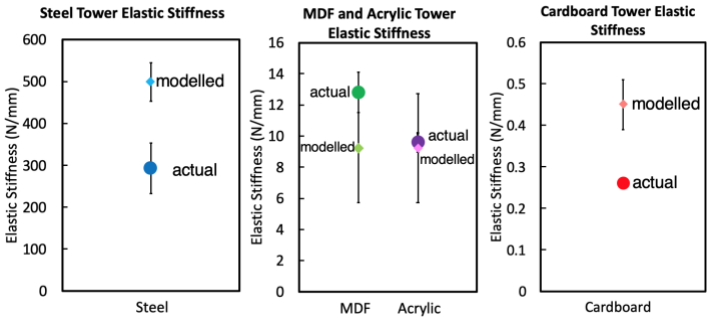

Figure 9: Three graphs of the modelled and actual tower stiffnesses for all materials. Note that the graphs are split because of the orders of magnitude differences from steel to MDF and acrylic to cardboard. The specific values and uncertainties of each of these graphs is summarized in Table 1. Also note that the error bars for the actual measured stiffness of the cardboard box are hidden behind the size of the marker.

To better visualize the materials compared to each other, a graph was made of the component stiffnesses as normalized to its respective tower stiffness. In this way, the relative relationship between the geometry and the stiffness may be compared for each of the materials on the same scale, as shown in Figure 10. Of note is that MDF, acrylic, and cardboard exhibit similar changes from tower to flexure and square, with the relative differences in those values roughly tracking the elastic stiffness of the material itself. Steel, however, shows substantially different behavior from this, with the square part being more stiff than the tower itself.

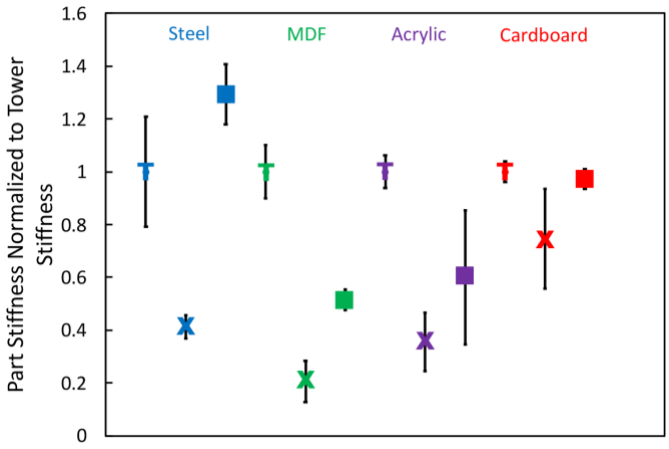

Figure 10: Comparison of the average measured tower, flexure component, and square component elastic stiffnesses as normalized to the tower stiffness for each material (steel, MDF, acrylic, and cardboard). Error bars are given by the scaled error of the non-normalized data. The T data marker indicates the tower, the X indicates the flexure, and the square indicates the square.

The measured tower stiffness vs. the predicted tower stiffness is graphed in Figure 11. This graph helps visualize the accuracy of the spring model, as a good model would generate a linear fit with a slope close to or equal to 1. In this case, the slope is 0.58 ± 0.02, which shows that across the four materials, the spring model on average over-predicts the actual value by 42%. While the proportional fit is statistically significant, which would suggest that the error in the model is systematically exacerbated by stiffer material types, this is likely a numerical artifact of fitting a line to a cluster of low stiffness points, and one point that is orders of magnitude larger than the others.

Because the steel data point dominates the fit because of its relative high stiffness, it is worth considering the measured tower stiffness vs. the predicted tower stiffness for only cardboard, acrylic and MDF, which is graphed in Figure 12. When excluding steel, the slope becomes 1.25 ± 0.33, which while it has a higher uncertainty than the steel fit, now overlaps with the accurate model slope of 1.

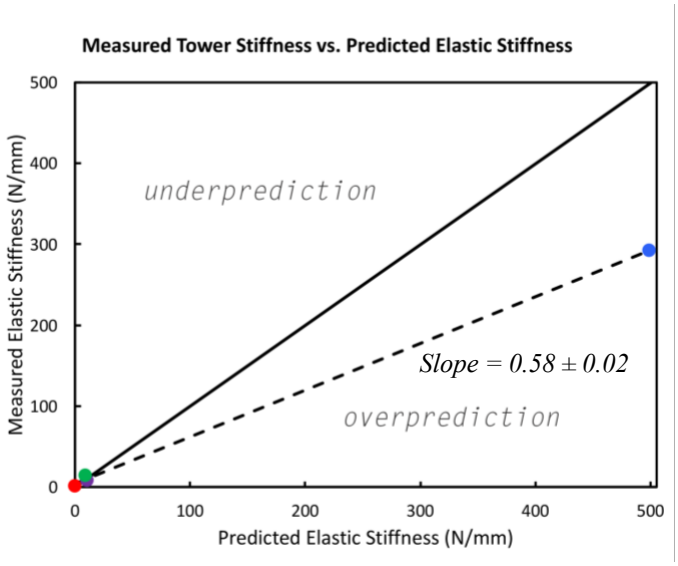

Figure 11: Graph of the measured tower stiffness (N/mm) versus the predicted or modelled tower stiffness (N/mm) for all of the materials. A linear fit of the measured values vs. the predicted values for a good model would have slope of 1. The slope here is 0.58 ± 0.02, which indicates that on average, the measured value is 58% that of the spring model.

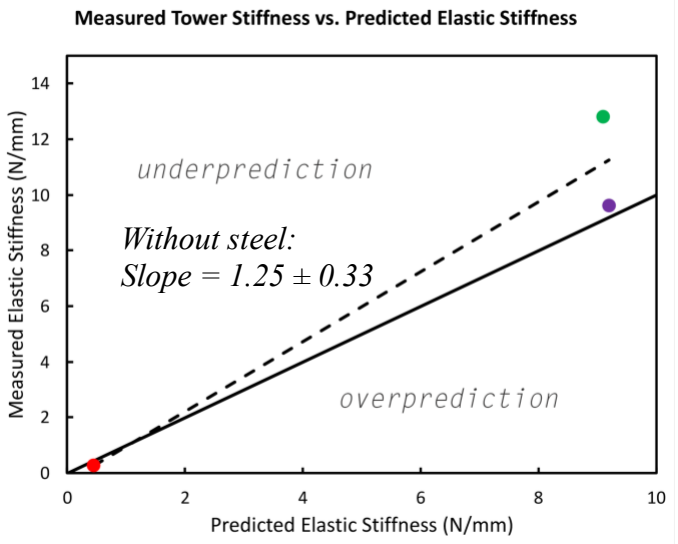

Figure 12: Graph of the measured tower stiffness (N/mm) versus the predicted or modelled tower stiffness (N/mm) for MDF, acrylic, and cardboard. The slope here is 1.25 ± 0.33, which overlaps with the accurate model slope of 1, indicating that the model is better able to predict behavior of the less stiff materials.

CONCLUSIONS

For MDF and acrylic, the spring model predicted tower stiffness overlaps with the measured tower stiffness. For acrylic specifically, the model predicts the tower

stiffness well, with a 4±14% undershoot of the actual value. However, the model is not able to predict the behavior of the steel and cardboard towers, as it overestimates the actual value by more than 70% in both cases. MDF and acrylic, the two materials for which the spring model is best able to predict behavior have similar elastic stiffnesses, which suggests that the simplified spring model may have limited use for materials within this range. To this end, future work should explore a range of materials more tightly clustered around the MDF/acrylic stiffness range (~1GPa-5GPa).

The most immediate reason why the spring model is unable to predict the stiffnesses of all of the towers is likely that it fails to take into consideration the cross linking components, which can impact the stiffness of the tower by constraining its ability to elastically deform in the directions perpendicular to the applied load. However, if this was the case, it would generally be expected then that the spring model under-predicts the stiffness of the tower instead of over-predicting it. This effect may cause the over-prediction nonetheless because compressive forces become more strongly concentrated in the joints of the tower. Further, design or assembly error could further exacerbate these stress concentrations. To see if the model fails because it is unable to account for stress concentrations in the joints of the tower, it would be worth testing other tower designs with varying amounts of additional joinery at the joints and seeing if this results in the measured tower stiffness better converging with the predicted one.

The mechanical properties of the material are more significant in determining the part and assembly behavior for less stiff materials. As can be seen from Figure 13, the less stiff materials have a tighter clustering of stiffnesses between the tower and component parts. To this end, future studies may want to more closely examine material types with stiffnesses in the range of steel, as compared to the other materials tested here, steel was the only material to have a measured tower stiffness that was lower than that of its square part stiffness. It would be additionally beneficial to know if the steel used here is an outlier in component stiffness as well as tower stiffness, as the measure of the model's accuracy is much better when steel is excluded.

While more work is needed to clarify the simplified spring model's validity for a range of materials, these results indicate that this model may be used to simplify the design process of a discrete assembly made of materials in the 1-5 GPa elastic stiffness range.

ACKNOWLEDGMENTS

Thanks to Dr. Kevin Cedrone and Dr. Barbara Hughey for all varieties of help with this project. Additional thanks to Pierce Hayward, Serena Do, and Sara Falcone for assistance with various physical aspects of this project.

REFERENCES

[1] Calisch, S., 2014, "Physical Finite Elements," S.M. thesis, Massachusetts Institute of Technology, Cambridge, MA, http://cba.mit.edu/docs/theses/14.08.Calisch.pdf.

[2] Hiller J., Lipson H., 2008, "Tunable Digital Material Properties for 3D Voxel Printers," Proceedings of the 19th Solid Freeform Fabrication Symposium, Austin TX.

[3] Nicholas B Cramer et al, "Elastic Shape Morphing of Ultralight…", 2019 Smart Mater. Struct. 28 055006, https://iopscience.iop.org/article/10.1088/1361-665X/ab0ea2/pdf.

[4] Calisch, S., et al "Fabrication and characterization of folded foils supporting streamwise travelling waves," IUTAM Symposium, June 18-22, 2018, Santorini Greece.

[5] Peek, N., 2010, "Rapid Prototyping of Green Composites," S.M. thesis, Massachusetts Institute of Technology, Cambridge, MA, http://cba.mit.edu/docs/theses/10.09.Peek.pdf.

[6]Cheung, K.C. 2012, "Digital Cellular Solids: Reconfigurable Composite Materials," Ph.D thesis, Massachusetts Institute of Technology, Cambridge, MA.

[7] Atlas Steels Australia, "Stainless Steel – Grade 304", datasheet, web, http://www.dm-consultancy.com/TR/dosya/1-59/h/aisi-340-info.pdf, (accessed 05/14/19).

[8] Design Technology, "Medium Density Fibreboard," https://design-technology.org/mdf.htm, (accessed 05/14/19).

[9]The Engineering Toolbox, "Young's Modulus," https://www.engineeringtoolbox.com/young-modulus-d_417.html, (accessed 05/14/19).

[10] ACME Plastics, "Acrylic," https://www.acmeplastics.com/content/advantages-acrylic/, (accessed 05/14/19).

[11] Fadiji, T., et al, n.d, "Investigating the Mechanical Properties of Paperboard…," Journal of Applied Packaging Research, https://scholarworks.rit.edu/cgi/viewcontent.cgi?referer=https://www.google.com/&httpsredir=1&article=1066&context=japr

[12] Instron, "Modulus of Elasticity," Instron Libr. [Online]. Available: http://www.instron.com/en-us/our-company/library/glossary/m/modulus-ofelasticity?region=North%20America. (Accessed: 28-Feb-2019).

[13] Sternheim, M., and Kane, J., "General Physics," 2nd edition, John Wiley and Sons, ISBN-10: 0471522783.

[14] Cheung, K. C., Gershenfeld, N., "Reversibly Assembled Cellular Composite Materials," Science, 341(6151):1219–1221.

[15] Schaedler, T., Jacobsen, A., and Carter, W., 2013, "Toward Lighter, Stiffer Materials," Science, 341(6151):11